

Diffraction by Dispersions of Spherical Membrane Vesicles. I. The Basic Equations

BY M. F. MOODY

Biology Department, Brookhaven National Laboratory, Upton, New York 11973, U.S.A.

(Received 20 March 1974; accepted 22 July 1974)

Equations are obtained for the coherent diffraction by a dispersion of spherical vesicles of different radii, where each vesicle is bounded by an identical membrane having negligible tangential structure. The diffraction pattern is compared with that given by an assemblage of flat sheets of the same membrane, and the two patterns are shown to differ significantly. The effects of membrane curvature thereby interfere with the determination of the membrane's structure; but, when correctly used, they might assist that determination.

1. Introduction

Dispersions of spherical vesicles are frequently obtained when membranes are prepared from cells or cell organelles, and also by the sonication of phospholipids. X-ray diffraction patterns of such preparations are an important potential source of information about cell membrane structure, and have been studied in recent years by various workers (Langridge, Barron & Sistrom, 1964; Chapman, Fluck, Penkett & Shipley, 1968; Wilkins, Blaurock & Engelman, 1971; Engelman, 1971; Lesslauer, Cain & Blasie, 1971, 1972; Blaurock, 1973). However, no exact theory relating the diffraction pattern of a dispersion of spherical vesicles to the structure of the membranous wall of each vesicle has apparently been developed.* Instead it has been generally assumed that such dispersions yield diffraction patterns which are virtually indistinguishable from those that would be given by isolated flat sheets of the same membrane. Although use of this approximation permits, in principle, analysis of the X-ray patterns when the membrane is believed to be symmetric† (Lesslauer, Cain & Blasie, 1971, 1972), it does not encourage the analysis of patterns from asymmetric membranes, into which category all natural lipoprotein membranes probably fall.

To avoid this difficulty, the dispersions can be made to give lamellar diffraction patterns when their membranes are flattened by drying or centrifugation (Finean, Coleman, Knutton, Limbrick & Thompson, 1968; Engelman, 1971; Dupont, Harrison & Hasselbach, 1973; Worthington & Liu, 1973). But, besides various technical problems inherent in these methods,

there is the possibility that the flattening procedure introduces artefacts – a possibility which might be tested by reference to the diffraction pattern of the original dispersion. It is therefore believed that useful information concerning membrane structure might still be obtained from dispersions, and that the best stimulus to obtain adequately precise diffraction data would be the existence of promising techniques for its analysis. As a foundation for developing such techniques, it is necessary to have an accurate and manageable theory of the diffraction by dispersions of spherical vesicles. The purpose of this paper is to develop such a theory, and to use it to assess the accuracy of the approximation referred to above, which will be shown to be significantly in error for certain parts of the diffraction pattern. Application of the theory to the problem of determining the structure of the vesicle membrane will be given in later publications.

2. Diffraction by an isolated vesicle

It is assumed that the vesicle is spherical and bounded by a uniform membrane of arbitrary (not necessarily symmetric) radial structure. By assuming that the membrane is uniform, we are supposing that the contributions of its tangential structure to the diffraction pattern are either negligible, or have been corrected for. (This question is examined in Appendix I.) Furthermore, it is assumed that the aqueous contents and surroundings of the vesicle have the same scattering density. (In practice this would almost always be true to within experimental error, since the vesicle walls would be too weak to support any significant difference in osmolarity between the inside and outside.)

Let the scattering density of the membrane (relative to the surrounding aqueous medium) be $\rho(u)$, and let that part of the membrane represented by $\rho(0)$ lie at a distance r from the center of the vesicle (Fig. 1). It will, on occasions, be useful to specify the origin $\rho(0)$ at different points with respect to the membrane, and r must of course change when a different origin is chosen.

* After this manuscript was submitted, there appeared an alternative theoretical study (Weick, 1974) of diffraction by hollow spherical membrane vesicles, treating the problem in direct space; but Weick considers only the case where the dispersion consists of vesicles with the same diameter.

† A *symmetric* membrane here means one with inside/outside symmetry, *i.e.* the scattering density ρ is an even function of the radial coordinate u ; $\rho(u) = \rho(-u)$ when the origin lies at the center of the membrane.

(Use of some defined origin will be denoted by attaching a subscript to ρ ; otherwise the origin is assumed to lie somewhere within the membrane.) With respect to its chosen origin, the transform of the membrane density is

$$G(R) = \int_{-\infty}^{\infty} \rho(u) \exp(2\pi i R u) du, \quad (1)$$

where the reciprocal-space coordinate $R = (2 \sin \theta) / \lambda$. Fig. 1 shows that a part of the membrane with coordinate u and density $\rho(u)$ lies at a radial distance $(r+u)$ from the center of the vesicle. Using the well-known expression for the transform of a spherically symmetric structure, the transform of a spherical vesicle is therefore

$$F(r, R) = (2/R) \int_{u_I}^{u_O} (r+u) \rho(u) \sin \{2\pi R(r+u)\} du.$$

The dependence of F on r expresses the fact that, for a given choice of origin of the membrane, changes in r denote changes in the radius of the vesicle. Unless the origin lies exactly at the inside surface of the membrane, u_I is negative but Fig. 1 shows that $r+u_I > 0$. Since $\rho(u) = 0$ when $u < u_I$ or $u > u_O$, the integration limits can be replaced by $-\infty$ and $+\infty$. Thus

$$\begin{aligned} F(r, R) &= (2/R) \int_{-\infty}^{\infty} (r+u) \rho(u) \sin \{2\pi R(r+u)\} du \\ &= \text{Im} (2/R) \int_{-\infty}^{\infty} (r+u) \rho(u) \exp \{2\pi i R(r+u)\} du \\ &= \text{Im} (2/R) \exp(2\pi i R r) \left[r \int_{-\infty}^{\infty} \rho(u) \right. \\ &\quad \left. \times \exp(2\pi i R u) du + \int_{-\infty}^{\infty} u \rho(u) \exp(2\pi i R u) du \right]; \end{aligned} \quad (2)$$

$\therefore F(r, R)$

$$= \text{Im} (2/R) \exp(2\pi i R r) [rG(R) + G'(R)/2\pi i], \quad (3)$$

where the prime denotes differentiation with respect to R . From a diffraction experiment we might hope to

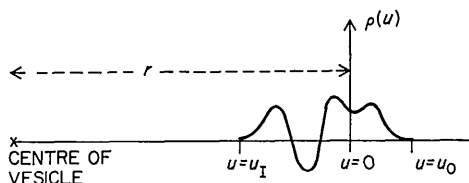


Fig. 1. Diagram of the coordinate frame used in deriving the transform of a spherical vesicle. An origin ($u=0$) is chosen somewhere within the membrane, whose scattering density (dark line) is $\rho(u)$. $\rho(u)$ is nonzero (*i.e.* the membrane scattering density differs from that of water) only when $u_I < u < u_O$. r is defined as the distance of the origin from the center of the vesicle.

determine $F^2(r, R)$, for which a convenient expression can be obtained as follows. Define

$$\begin{aligned} H(r, R) &= (2/R) \exp(2\pi i R r) [rG(R) + G'(R)/2\pi i] \\ &= E(r, R) + iF(r, R), \end{aligned} \quad (4)$$

where both E and F are real functions. Then

$$\begin{aligned} F^2(r, R) &= \frac{1}{2}[E^2(r, R) + F^2(r, R)] - \frac{1}{2}[E^2(r, R) - F^2(r, R)] \\ &= \frac{1}{2}|H(r, R)|^2 - \frac{1}{2}\text{Re} \{H^2(r, R)\}. \end{aligned} \quad (5)$$

Before proceeding further, it is helpful to gain some qualitative insight into the behavior of the two terms on the right-hand side of equation (5). We begin with the first term which, by equation (4), is $(2/R^2)|rG(R) + G'(R)/2\pi i|^2$ and is consequently always positive. By equation (1) this expression is

$$(2/R^2) \left| \int_{-\infty}^{\infty} (r+u) \rho(u) \exp(2\pi i R u) du \right|^2,$$

and is unaffected by our choice of the origin of ρ . If we choose it to lie at the middle of the membrane (of thickness $u_O - u_I$), then

$$\frac{1}{2}|H(r, R)|^2 = (2/R^2) \left| \int_{u_I}^{u_O} (r+u) \rho(u) \exp(2\pi i R u) du \right|^2.$$

The Fourier component of this term with the highest frequency is $\cos 2\pi R(u_O - u_I)$, and the term as a whole cannot vary much faster than this.

The second term, $\frac{1}{2}\text{Re} \{H^2(r, R)\}$, can be regarded (see Fig. 2) as the projection of a vector whose length [by equation (4)] is $(2/R^2)|rG(R) + G'(R)/2\pi i|^2$, and whose phase is $4\pi R + 2 \cdot \arg \{rG(R) + G'(R)/2\pi i\}$. Consider the rapidity with which this vector moves, relative to the line OA . The angle between these lines is $2 \cdot \arg \{rG(R) + G'(R)/2\pi i\}$ which, by equation (1), is

$$2 \cdot \arg \left\{ \int_{-\infty}^{\infty} (r+u) \rho(u) \exp(2\pi i R u) du \right\}.$$

The origin of ρ is supposed to lie somewhere within the membrane, so this term will change most rapidly when the origin is chosen to lie at one surface of the membrane. In that case the highest-frequency Fourier components of the integral are

$$\frac{\sin}{\cos} \{2\pi R(u_O - u_I)\}.$$

Thus, apart from occasional rapid 180° changes of phase (which occur only when both the real and imaginary parts of $H^2(r, R)$ are small), the angle between the vector and OA will not change (as a function of R) more rapidly than $4\pi R(u_O - u_I)$. The angle between OA and the coordinate frame, however, is $4\pi R r$; and this changes much more rapidly with R , since the vesicle radius r is substantially larger than the membrane thickness $(u_O - u_I)$. Now if the angle between OA and the vector were fixed, its projection $\frac{1}{2}\text{Re} \{H^2(r, R)\}$ would be a cosine wave of high (constant) frequency. Because of the changes in length and angle (relative to OA) of the vector, this cosine wave will be modulated in amplitude and phase; but these modulations will,

as we have seen, be slow in comparison with the high 'carrier' frequency of the cosine wave.

In summary, the first term on the right of equation (5) is positive and changes relatively slowly with R . The second term, however, oscillates rapidly like a cosine wave of relatively high (but slowly modulated) frequency, and amplitude prescribed by the first term.

3. Diffraction from a dispersion of vesicles of different radii

We assume that the vesicles, though of different size, are composed of membranes of identical structure, and are randomly distributed in such a way that inter-particle interference effects (which would in any case be reduced by polydispersity) can be ignored. Then the corrected intensity $I(R)$ will represent the incoherent sum of the photons scattered from each vesicle. To calculate this intensity we need to define a function that describes the size distribution of the vesicles. Let $p(r)dr$ represent the fraction of vesicles whose radius (measured out to whatever origin is chosen within the membrane) lies between r and $r+dr$. $p(r)$ can be regarded as a probability density function with mean $\langle r \rangle$, variance $\sigma^2(r)$, and whose characteristic function

$$P(X) = \int_{-\infty}^{\infty} p(r) \exp(iXr) dr. \quad (6)$$

The corrected intensity is now

$$I(R) \propto \int_0^{\infty} p(r) F^2(r, R) dr, \quad (7)$$

so

$$I(R) \propto \int_0^{\infty} p(r) |H(r, R)|^2 dr - \text{Re} \int_0^{\infty} p(r) H^2(r, R) dr. \quad (8)$$

Even without examining the integrals in detail, their qualitative behavior is fairly clear. Since $|H(r, R)|^2$ is positive and changes only rather slowly with respect to R , the smearing effect of $p(r)$ will not change it drastically. But the rapidly oscillating function $\text{Re} \{H^2(r, R)\}$ will, by the principle of stationary phase, be annihilated (except very near the origin of R) by a broad and smooth function $p(r)$, in which case the scattering will (except at very low angles) relate exclusively to the first integral [Atkinson, Hauser, Shipley & Stubbs (1974) give model calculations illustrating this effect]. A more detailed analysis of each integral now follows.

4. Fine-fringe component in diffraction by dispersions

As explained in § 2, $\text{Re} \{H^2(r, R)\}$ represents a component of $F^2(r, R)$ consisting of fine fringes whose spacing relates to the radius of the vesicle. The second term of equation (8), $\text{Re} \int_0^{\infty} p(r) H^2(r, R) dr$, represents this fine-fringe component smeared by the size distribution

function $p(r)$. Since r is the distance from the center of the vesicle to some chosen origin within the membrane, $p(r)=0$ when r is negative; consequently the lower limit of integration can be extended to $-\infty$. Then

$$\begin{aligned} \text{Re} \int_0^{\infty} p(r) H^2(r, R) dr &= \frac{4}{R^2} \text{Re} \int_{-\infty}^{\infty} p(r) \\ &\times \exp(4\pi i r R) [rG(R) + G'(R)/2\pi i]^2 dr. \end{aligned}$$

Expansion of the square and use of equation (6) gives

$$\begin{aligned} \text{Re} \int_0^{\infty} p(r) H^2(r, R) dr &= \frac{-1}{(2\pi R)^2} \text{Re} \left[G^2(R) \frac{d^2}{dR^2} P(4\pi R) \right. \\ &\left. + 4G(R)G'(R) \frac{d}{dR} P(4\pi R) + 4\{G'(R)\}^2 P(4\pi R) \right]. \end{aligned} \quad (9)$$

If the distribution function $p(r)$ is smooth and broad, its transform $P(4\pi R)$ will be negligible unless R is small. The same applies to the first two derivatives of $P(4\pi R)$. For example, if $p(r)$ has (approximately) the form of the normal distribution, *i.e.* if

$$p(r) \doteq (\sigma\sqrt{2\pi})^{-1} \exp[-(r-\langle r \rangle)^2/2\sigma^2], \quad (10)$$

then

$$P(4\pi R) \doteq \exp(4\pi i R \langle r \rangle) \exp(-8\pi^2 \sigma^2 R^2) \quad (11)$$

and all the derivatives contain $P(4\pi R)$ as a factor. Consequently $P(4\pi R)$ and its first two derivatives become negligible when $R\sigma \gtrsim 0.3$. Thus in most cases the fine-fringe component vanishes except at very low angles (as expected). However, exceptions may occur if the vesicle size, or merely the lower limit of this size, were rather precisely determined by biological or physical factors.

When the diffraction pattern shows even a very few fine fringes near the origin, useful information can be obtained concerning the size distribution of the vesicles. Thus Langridge, Barron & Siström (1964) cal-

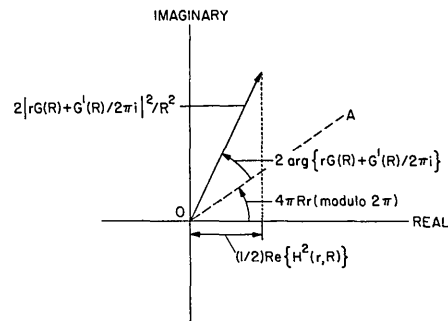


Fig. 2. Representation of $\frac{1}{2} \text{Re} \{H^2(r, R)\}$ as the projection of a vector in the Argand diagram.

culated, from such data, a mean radius of 295 Å; and, from the disappearance of the fringes at $R \doteq \frac{1}{1.20} \text{ Å}^{-1}$, the criterion $R\sigma \doteq 0.3$ gives us the rough estimate $\sigma \doteq 35 \text{ Å}$.

5. Slowly modulated component in diffraction by dispersions

We now evaluate the first term on the right-hand side of equation (8).

$$\int_0^\infty p(r)|H(r, R)|^2 dr = \frac{4}{R^2} \int_0^\infty p(r)|rG(R) + G'(R)/2\pi i|^2 dr$$

by equation (4);

$$\begin{aligned} &= \frac{4}{R^2} \int_0^\infty p(r) \left[r^2 |G(R)|^2 + 2r \operatorname{Re} \left\{ G^*(R) \frac{G'(R)}{2\pi i} \right\} \right. \\ &\quad \left. + |G'(R)/2\pi i|^2 \right] dr \\ &= \frac{4}{R^2} \left[\langle r^2 \rangle |G(R)|^2 + 2\langle r \rangle \operatorname{Re} \left\{ G^*(R) \frac{G'(R)}{2\pi i} \right\} \right. \\ &\quad \left. + |G'(R)/2\pi i|^2 \right], \end{aligned}$$

where

$$\langle r^k \rangle = \int_{-\infty}^\infty r^k p(r) dr = \int_0^\infty r^k p(r) dr, \quad (12)$$

since $p(r) = 0$ when $r \leq 0$. Finally, by using the formula

$$\langle r^2 \rangle = \langle r \rangle^2 + \sigma^2(r), \quad (13)$$

we obtain the surprisingly simple result

$$\int_0^\infty p(r)|H(r, R)|^2 dr = \frac{4}{R^2} \left[\langle r \rangle G(R) + G'(R)/2\pi i \right]^2 + |G(R)|^2 \sigma^2(R). \quad (14)$$

This is an important formula since, in most practical cases, the diffraction pattern (except possibly at very low angles) relates exclusively to this term of equation (8).

6. Validity of the 'flat sheet' approximation

All previous quantitative analyses of X-ray data from inhomogeneous dispersions of spherical vesicles have adopted what is here termed the 'flat sheet' approximation. According to this, the diffraction pattern (outside those very low angles where there may be fine fringes relating to the vesicle diameters) is the same as that of a random assemblage of flat sheets of the vesicle membrane. Using the exact equation (14) for the diffracted intensity when the fine-fringe component is negligible, the 'flat sheet' approximation is

$$|\langle r \rangle G(R) + G'(R)/2\pi i|^2 + |G(R)|^2 \sigma^2(r) \propto |G(R)|^2,$$

approximately. Clearly this is accurate when either

$\langle r \rangle \rightarrow \infty$ or $\sigma^2(r) \rightarrow \infty$, as is only reasonable since in either case the overwhelming proportion of vesicles have essentially flat membranes. In practice, however, the membrane thickness (50–100 Å) is not negligible in comparison with $\langle r \rangle$ (100–500 Å).

The ideal way to investigate deviations from the 'flat sheet' approximation in such cases would be to adjust k so as to minimize

$$\int_0^\infty \{ |\langle r \rangle G(R) + G'(R)/2\pi i|^2 + |G(R)|^2 \sigma^2(r) - k |G(R)|^2 \}^2 dR,$$

and then to consider the minimum value of this integral. Unfortunately, this approach proves mathematically intractable. But an approximate estimate of the contribution of $G'(R)/2\pi i$ to the diffraction pattern can be obtained from the arguments presented in Appendix II. There it is shown that, for a just comparison of $G(R)$ and $G'(R)/2\pi i$, the origin of $\varrho(u)$ should be chosen to lie at the center of mass of $\varrho^2(u)$ and that, with this origin choice (symbolized by use of the subscript C), the fractional contribution of $G'_C(R)/2\pi i$ to any part of the diffraction pattern could be expected to be about $4\gamma \langle r_C \rangle / \pi \langle r_C^2 \rangle$. In many cases this approaches 10%; so, while it would be negligible in some parts of the pattern, in other parts it would make a contribution of the order of up to 10% of the average value of $|G_C(R)|$.

Such a contribution is quite significant when $|G_C(R)|$ happens to be smaller than average. Now $G'_C(R)/2\pi i$ is often at its largest where $G_C(R)$ is at its smallest, so the effect of $G'_C(R)/2\pi i$ (and hence of the membrane curvature) on the diffraction pattern is much greater than would be suggested by equation (II. 9). This uneven distribution of the effect is most clearly apparent in the case of vesicles bounded by a symmetric membrane, *i.e.* by one for which $\varrho_C(u) = \varrho_C(-u)$. $G_C(R)$ is then real, so that $G'_C(R)$ [and hence $G'_C(R)/2\pi i$] is zero at the peaks of $G_C(R)$. As Fig. 3 shows, this has the effect that the positions and heights of the maxima correspond to those predicted by the 'flat sheet' approximation. The contribution due to membrane curvature is mainly concentrated around those minima of $G_C(R)$ where it changes sign, since $G'_C(R)$ is then particularly large. Now the $G'_C(R)/2\pi i$ vector is always perpendicular to the $G_C(R)$ vector (since the former quantity is a pure imaginary, and the latter a pure real, for a symmetric membrane), so the contribution of $G'_C(R)/2\pi i$ always increases $I(R)$. Thus $G'_C(R)/2\pi i$ partly fills those minima that lie at nodes of the transform $G(R)$, as shown in Fig. 3. Consequently the diffracted intensity can never fall to zero, a fact observed experimentally by Wilkins, Blaurock & Engelman (1971). Thus membrane curvature has the effect of obscuring the difference between those minima that lie at transform nodes, and those that do not. The process of phasing the pattern from the course of the intensity curve is thereby hindered, making the phases quite unreliable unless the effects of membrane curvature are taken into account.

With a symmetric membrane, then, the effects of membrane curvature are significant only in the neighborhood of a node of the transform $G_c(R)$. Elsewhere $\langle r_c \rangle G_c(R)$ is substantially larger than $G'_c(R)/2\pi i$ and, since the two vectors are orthogonal, the latter causes very little increase in the modulus of their sum. When the membrane is asymmetric, however, the situation is somewhat different. $G_c(R)$ is complex and has no nodes, so it is unlikely that there will be any regions where $|G'_c(R)/2\pi i| > |G_c(R)|$. In most places it will be substantially smaller than $|G_c(R)|$, so that only the component of the $G'_c(R)/2\pi i$ vector that is parallel (or antiparallel) to the $G_c(R)$ vector will significantly affect $I(R)$. The effect of $G'_c(R)/2\pi i$ will thus be greatest when the two vectors are parallel (or antiparallel), which occurs at stationary points* of $|G_c(R)|^2$. At the maxima of $|G_c(R)|^2$, however, the effect will be only small, for most of these maxima occur where both the real and imaginary parts of $G_c(R)$ are fairly near their own maxima, and are thus not changing rapidly. Consequently the largest effect is to be expected at the minima of $|G_c(R)|^2$, *i.e.* near the minima of $I(R)$, as seen in Fig. 4. The contribution of membrane asymmetry to enhancing the effects of membrane curvature can be appreciated by comparing the first vesicle diffraction pattern (continuous curve in Fig. 4) with that given by vesicles with the same size distribution and membrane structure, but turned inside-out (dotted curve in Fig. 4). The curve representing the intensity on the 'flat sheet' approximation (broken curve in Fig. 4) nearly bisects the other two curves, showing that most of the effects of membrane curvature would vanish if the two curves coincided through disappearance of the membrane asymmetry. This approximate bisection of the two curves can be understood as follows. The effect of $G'_c(R)/2\pi i$ depends, as we have seen, largely on its component parallel to the $G_c(R)$ vector, *i.e.* on the magnitude of the scalar product of the two vectors (considered as ordinary two-dimensional vectors). When the orientation of the membrane is reversed, $\text{Im}\{G_c(R)\}$ and $\text{Re}\{G'_c(R)/2\pi i\}$ change their signs while the other two parts remain the same. Consequently the scalar product of the corresponding two-dimensional vectors changes sign, and the change in $I(R)$ is approximately reversed.

In summary, the 'flat sheet' approximation can be expected (for most vesicle sizes) to be significantly in error in certain parts (particularly around the troughs) of the diffraction pattern. This error need not be tolerated, since the exact equation (14) is little more complicated to use than is the approximation itself. A second and more important conclusion of the foregoing discussion is that the contribution of $G'_c(R)/2\pi i$

* At stationary values of $|G(R)|^2$, $0 = (d/dR)|G(R)|^2 = (d/dR)[G_r^2(R) + G_i^2(R)]$, writing $G_r(R)$ and $G_i(R)$ respectively for the real and imaginary parts of $G(R)$. Hence $G_r(R)G'_i(R) + G_i(R)G'_r(R) = 0$, so the $G(R)$ vector in the Argand diagram is orthogonal to the $G'(R)$ vector, and therefore parallel or antiparallel to the $G'(R)/2\pi i$ vector.

should be easily detectable in some parts of a typical diffraction pattern. This is potentially of value in determining the structure of the vesicle membrane. For example, Fig. 4 shows that the diffraction pattern of vesicles with an asymmetric membrane is sensitive to the direction of the membrane asymmetry, and

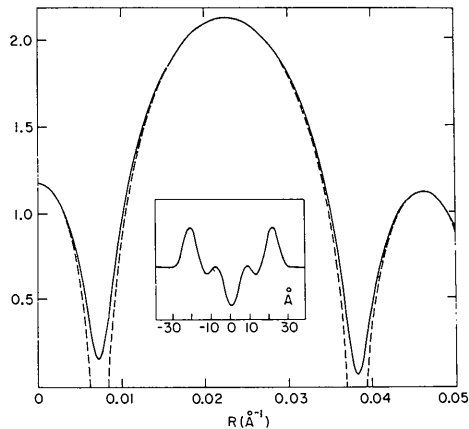


Fig. 3. A plot of $\log_{10}\{I(R) \cdot R^2\}$ against R , where $I(R)$ is the intensity of diffraction at a reciprocal spacing $R(\text{\AA}^{-1})$ from a dispersion in which the vesicle membrane is symmetric. The membrane density (insert) is that for a phospholipid bilayer (Lesslauer *et al.*, 1971). The vesicle dimensions correspond with those of the fraction II liposomes of Huang (1969): $\langle r_c \rangle = 125 \text{\AA}$ (implying a mean outer diameter of $\sim 300 \text{\AA}$), and $\sigma(r) = 10 \text{\AA}$. Solid line – correct intensity for dispersion (omitting any fine fringes); broken line – intensity given by a random assemblage of flat sheets with the same membrane structure.

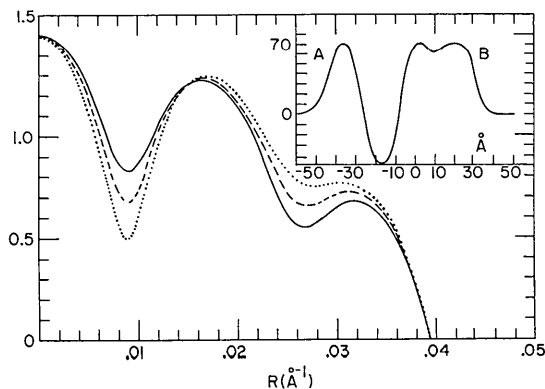


Fig. 4. A plot of $\log_{10}\{I(R) \cdot R^2\}$ against R , where $I(R)$ is the intensity of diffraction at a reciprocal spacing $R(\text{\AA}^{-1})$ from a dispersion in which the vesicle membrane is asymmetric. The membrane density (insert) is hypothetical. The vesicle dimensions correspond approximately with those of the chromatophores studied by Langridge *et al.* (1964): $\langle r_c \rangle = 300 \text{\AA}$ (implying a mean outer diameter of $\sim 690 \text{\AA}$), and $\sigma(r) = 35 \text{\AA}$. The fine-fringe term (negligible for $R \gtrsim 1/100 \text{\AA}$) is omitted. Solid line – correct intensity for the dispersion with center of vesicles on side A of the membrane; dotted line – as above, but with center of vesicles on side B; broken line – intensity given by a random assemblage of flat sheets with the same membrane structure.

could therefore provide evidence concerning the orientation of the membrane in the vesicle. Furthermore, when the membrane is symmetric, the intensity minima which occur at nodes of the membrane transform might be distinguished from those that do not by the sensitivity of the former to the mean vesicle diameter. These and other applications of the theory developed in this paper will be examined in later publications.

Research carried out at Brookhaven National Laboratory under the auspices of the U.S. Atomic Energy Commission and also supported by a grant (AI 11585) from the National Institutes of Health.

APPENDIX I

Effect of tangential membrane structure on the diffraction pattern of dispersions

If the vesicle membrane contains significant tangential structure, we must replace $\varrho(r)$ by $\varrho(r, \theta, \varphi)$, where r is now the radial coordinate and (r, θ, φ) are spherical polar coordinates, θ measuring the angle from the z axis. If we now define

$$f_{n,m}(r) = \frac{1}{4\pi} \int_0^\pi \sin \theta P_n^m(\cos \theta) \left[\int_0^{2\pi} \varrho(r, \theta, \varphi) \times \exp(-im\varphi) d\varphi \right] d\theta, \quad (\text{I.1})$$

where $P_n^m(x)$ is an associated Legendre function, then $f_{0,0}$ represents the spherically symmetrical density $\varrho(r)$ used in this paper. The Fourier transform of the vesicle density is now denoted by $F(R, \Theta, \Phi)$, where (R, Θ, Φ) are the spherical polar coordinates of reciprocal space. However, the diffraction pattern of an isolated vesicle would relate to

$$\langle F(R, \Theta, \Phi)^2 \rangle_{\Theta, \Phi} = \frac{1}{4\pi} \int_0^\pi \sin \Theta \left[\int_0^{2\pi} |F(R, \Theta, \Phi)|^2 d\Phi \right] d\Theta. \quad (\text{I.2})$$

Harrison (1967, 1969) has shown that

$$\langle F(R, \Theta, \Phi)^2 \rangle_{\Theta, \Phi} = \left[\frac{2}{R} \int_0^\infty r f_{0,0}(r) \sin(2\pi Rr) dr \right]^2 + \sum_{n=0}^{\infty} \left[\sum_{m=-n}^n (16\pi^2 c_{n,m})^{-1} \int_0^\infty r^2 f_{n,m}(r) j_n(2\pi Rr) dr \right]^2, \quad (\text{I.3})$$

where

$$c_{n,m} = \frac{(n+m)!}{(n-m)!} \frac{1}{2n+1}$$

and $j_n(x)$ is a spherical Bessel function. (This equation represents the application of Parseval's theorem to the angular components of spherical harmonics, in terms of which the Fourier transform is being expressed.) When we consider a dispersion of vesicles with different radii, the above equation must be averaged with respect

to the size distribution function $p(r)$. Although this paper is concerned only with the averaging of the first term alone, it is clear from the above equation that the averaging of that term will not be changed when the entire series is averaged with respect to $p(r)$. Thus, if the remainder of the averaged series could be determined, it would be possible to subtract it from the corrected intensity, obtaining the quantity, $\int_0^\infty p(r) F^2(r, R) dr$, which is investigated in this paper. A rough estimate of this remainder can be obtained from the diffraction pattern of preparations in which the spherical averaging has been circumvented by drying or centrifugation (Finean, Coleman, Knutton, Limbrick & Thompson, 1968; Engelman, 1971; Dupont, Harrison & Hasselbach, 1973; Worthington & Liu, 1973). In such preparations the tangential structure makes only a minor contribution to the X-ray pattern (Fig. 2 of Worthington & Liu, 1973), particularly when it is remembered that the edges of a flattened vesicle will contribute to that region of an X-ray pattern where evidence for tangential structure is sought. The relative insignificance of the tangential structure is also apparent in the diffraction patterns of oriented lamellar membrane systems such as synthetic multilayers (Levine & Wilkins, 1971), nerve myelin (Schmitt, Bear & Clark, 1935) and the discs of rod outer segments (Blaurock & Wilkins, 1969).

APPENDIX II

Size of the contribution of the term $G'(R)/2\pi i$ to the diffraction pattern

First we shall investigate the relative magnitudes of $G(R)$ and $G'(R)/2\pi i$ and then discuss the size of the latter term's contribution to the diffraction pattern of a dispersion of vesicles, considering the case when the intensity is essentially given by equation (14).

When we try to compare the magnitudes of $G(R)$ and $G'(R)/2\pi i$ we immediately encounter the problem that the result depends on our choice of the origin of the membrane density $\varrho(u)$. Consider the case of an isolated spherical vesicle. Suppose we first choose the origin to lie at some part of the membrane which is at a distance r_1 from the center of the vesicle, and that we calculate by equation (1) the functions $G_1(R)$ and $G'_1(R)/2\pi i$. If we next choose the origin at some different part of the membrane at a radius r_2 , we have $\varrho_2(u) = \varrho_1(r_2 - r_1 + u)$, and we now calculate

$$G_2(R) = \exp[2\pi i R(r_1 - r_2)] G_1(R) \quad (\text{II.1})$$

and

$$\begin{aligned} & G'_2(R)/2\pi i \\ &= \exp[2\pi i R(r_1 - r_2)] \{ G'_1(R)/2\pi i + (r_1 - r_2) G_1(R) \}. \quad (\text{II.2}) \end{aligned}$$

Although the diffracted intensity calculated from equation (14) is (as we should require) the same with either origin, the relative magnitudes of $G(R)$ and $G'(R)/2\pi i$

change as the latter quantity acquires or loses some component of the former on displacement of the origin. Since this component obeys the 'flat sheet' approximation exactly, we might be misled into exaggerating the inaccuracy of that approximation if we were to choose the origin incorrectly.

We should thus choose the origin so as to minimize or eliminate the component of $G(R)$ contained in $G'(R)/2\pi i$. For this purpose we can calculate the correlation

$$Q = \int_0^\infty G^*(R) \frac{G'(R)}{2\pi i} dR \quad (\text{II.3})$$

as a function of the position of the origin, and proceed to minimize Q . It is shown in Appendix III that

$$Q = \frac{1}{2} \int_{-\infty}^\infty u \varrho^2(u) du + (i/4\pi) \left[\int_{-\infty}^\infty \varrho(u) du \right]^2. \quad (\text{II.4})$$

The imaginary part of Q is independent of the choice of origin. (This part vanishes if the lower integration limit in equation (II.3) is extended to $-\infty$). More important is the real part, which measures the integral of the scalar product of $G(R)$ and $G'(R)/2\pi i$, each being represented as a two-dimensional vector in the Argand diagram. By equation (II.4) the real part can be made to disappear if the origin of $\varrho(u)$ is placed at the center of mass of $\varrho^2(u)$, a choice of origin that will be indicated by the subscript C on all relevant quantities. When the origin of ϱ is chosen in this way, $G'_C(R)/2\pi i$ is uncorrelated with $G_C(R)$, and it should be at least approximately true that the contribution of the term $G'(R)/2\pi i$ to the diffraction pattern is minimized. Moreover, when $G'(R)/2\pi i$ has this minimum value, its contribution to the expression $|\langle r \rangle G_C(R) + G'_C(R)/2\pi i|^2 + |G_C(R)|^2 \sigma^2(r)$ should give an approximate measure of the deviation of that expression from the 'flat sheet' approximation.

Proceeding on these assumptions, we now calculate the contribution of $G'_C(R)/2\pi i$ to the total diffraction pattern. From equations (8) and (14)

$$\begin{aligned} & \int_0^\infty I(R) R^2 dR \propto \int_0^\infty |\langle r_C \rangle G_C(R) + G'_C(R)/2\pi i|^2 dR \\ & + \sigma^2(r) \int_0^\infty |G_C(R)|^2 dR \propto [\langle r_C \rangle^2 + \sigma^2(r)] \\ & \times \int_0^\infty |G_C(R)|^2 dR + 2\langle r_C \rangle \text{Re} \left[\int_0^\infty G_C^*(R) \frac{G'_C(R)}{2\pi i} dR \right] \\ & + \int_0^\infty \left| \frac{G'_C(R)}{2\pi i} \right|^2 dR \\ & \propto \langle r_C^2 \rangle \int_0^\infty |G_C(R)|^2 dR + \int_0^\infty \left| \frac{G'_C(R)}{2\pi i} \right|^2 dr \quad (\text{II.5}) \end{aligned}$$

by equations (13) and (II.4).

Thus an approximate measure of the mean fractional error of the 'flat sheet' approximation is

$$\alpha = \int_0^\infty |G'_C(R)/2\pi i|^2 dR / \{ \langle r_C^2 \rangle \int_0^\infty |G_C(R)|^2 dR \}. \quad (\text{II.6})$$

Since $|G_C(R)|^2$ is an even function,

$$\begin{aligned} & \int_0^\infty |G_C(R)|^2 dR \\ & = \frac{1}{2} \int_{-\infty}^\infty |G_C(R)|^2 dR = \frac{1}{2} \int_{-\infty}^\infty \varrho^2(u) du, \quad (\text{II.7}) \end{aligned}$$

by applying Parseval's theorem to equation (1). Similarly,

$$\begin{aligned} & \int_0^\infty |G'_C(R)/2\pi i|^2 dR \\ & = \frac{1}{2} \int_{-\infty}^\infty |G'_C(R)/2\pi i|^2 dR = \frac{1}{2} \int_{-\infty}^\infty u^2 \varrho_C^2(u) du. \quad (\text{II.8}) \end{aligned}$$

Equation (II.5) now gives the estimated mean fractional error as

$$\alpha = \gamma^2 / \langle r_C^2 \rangle \quad (\text{II.9})$$

where γ is the one-dimensional 'radius of gyration' of the squared membrane density, *i.e.* where

$$\gamma^2 = \int_{-\infty}^\infty u^2 \varrho_C^2(u) du / \int_{-\infty}^\infty \varrho_C^2(u) du. \quad (\text{II.10})$$

The estimated mean fractional error α , by equation (II.9), is in most cases only a few percent or less, so the overall contribution of $G'(R)/2\pi i$ is quite small. But we must now investigate its distribution, *i.e.* how large we might expect that contribution to be at any part of the diffraction pattern. From equations (II.6) and (II.9) we can suppose that $|G'_C(R)/2\pi i|^2$ has a typical value of about $\gamma^2 |G_C(R)|^2$, *i.e.* that $|G'_C(R)/2\pi i|$ has a typical value of about $\gamma |G_C(R)|$. If the phase angle between the $G_C(R)$ and $G'_C(R)/2\pi i$ vectors in the Argand diagram is ω , then $|\langle r_C \rangle G_C(R) + G'_C(R)/2\pi i|^2$ has the typical value of about $|G_C(R)|^2 (\langle r_C \rangle^2 + 2\langle r_C \rangle \gamma \cos \omega + \gamma^2)$. Now, as we have seen, the integral and hence the average of the scalar product of the $G_C(R)$ and $G'_C(R)/2\pi i$ vectors is zero, *i.e.* the average value of $\cos \omega$ is zero. Since ω generally passes through all angles, a typical value of $\cos \omega$ will be $\pm 2/\pi$. Neglecting γ^2 in comparison with $\langle r_C \rangle^2$ or $2\langle r_C \rangle \gamma \cos \omega$, the fractional contribution of $G'_C(R)/2\pi i$ to any part of the diffraction pattern could therefore be expected to be about $4\gamma \langle r_C \rangle / \pi \langle r_C^2 \rangle$.

APPENDIX III

Evaluation of an integral

It is required to evaluate

$$Q = \int_0^\infty G^*(R) \frac{G'(R)}{2\pi i} dR.$$

We can write $Q = \frac{1}{2}(Q + Q^*) + \frac{1}{2}(Q - Q^*)$, where the first two terms on the right constitute its real, and the last two its imaginary part. Both $G(R)$ and $G'(R)/2\pi i$ have Hermitian symmetry, since they are Fourier transforms of the real functions $q(u)$ and $uq(u)$, respectively. Consequently

$$\begin{aligned} Q &= \frac{1}{2} \int_0^\infty G(-R) \frac{G'(R)}{2\pi i} dR + \frac{1}{2} \int_0^\infty G(R) \frac{G'(-R)}{2\pi i} dR \\ &+ \frac{1}{2} \int_0^\infty [G(-R)G'(R)/2\pi i - G(R)G'(-R)/2\pi i] dR \\ &= -\frac{1}{2} \int_0^\infty G(S) \frac{G'(-S)}{2\pi i} dS \\ &+ \frac{1}{2} \int_0^\infty G(R) \frac{G'(-R)}{2\pi i} dR + \frac{1}{4\pi i} \int_0^\infty \frac{d}{dR} \\ &\quad \times [G(-R)G(R)] dR \\ &= \frac{1}{2} \int_{-\infty}^\infty G(R) \frac{G'(-R)}{2\pi i} dR - \frac{i}{4\pi} [G(R)]_{R=0}^{R=\infty} \\ &= \frac{1}{2} \int_{-\infty}^\infty G(R) \frac{G'(-R)}{2\pi i} \exp(-2\pi i R x) dr \Big|_{x=0} \\ &+ iG^2(0)/4\pi, \end{aligned}$$

since $|G(\infty)|^2 = 0$.

By the convolution theorem, the integral is the convolution of the transforms of $G(R)$ and of $G'(R)/2\pi i$, i.e.

$$Q = \frac{1}{2} \int_{-\infty}^\infty q(u) (u-x)q(u-x) du \Big|_{x=0} + iG^2(0)/4\pi.$$

$$\therefore Q = \frac{1}{2} \int_{-\infty}^\infty uq^2(u) du + (i/4\pi) \left[\int_{-\infty}^\infty q(u) du \right]^2.$$

References

- ATKINSON, D., HAUSER, H., SHIPLEY, G. G. & STUBBS, J. M. (1974). *Biochim. Biophys. Acta.* **339**, 10–29.
- BLAUROCK, A. E. (1973). *Biophys. J.* **13**, 290–298.
- BLAUROCK, A. E. & WILKINS, M. H. F. (1969). *Nature, Lond.* **223**, 906–909.
- CHAPMAN, D., FLUCK, D. J., PENKETT, S. A. & SHIPLEY, G. G. (1968). *Biochim. Biophys. Acta*, **163**, 255–261.
- DUPONT, Y., HARRISON, S. C. & HASSELBACH, W. (1973). *Nature, Lond.* **244**, 555–558.
- ENGELMAN, D. M. (1971). *J. Mol. Biol.* **58**, 153–165.
- FINEAN, J. B., COLEMAN, R., KNUITON, S., LIMBRICK, A. R. & THOMPSON, J. E. (1968). *J. Gen. Physiol.* **51**, 195–255.
- HARRISON, S. C. (1967). *The Structure of Tomato Bushy Stunt Virus*. Ph.D. Thesis, Harvard Univ.
- HARRISON, S. C. (1969). *J. Mol. Biol.* **42**, 457–483.
- HUANG, C. (1969). *Biochemistry*, **8**, 344–352.
- LANGRIDGE, R., BARRON, P. D. & SISTROM, W. R. (1964). *Nature, Lond.* **204**, 97–98.
- LESSLAUER, W., CAIN, J. & BLASIE, J. K. (1971). *Biochim. Biophys. Acta*, **241**, 547–566.
- LESSLAUER, W., CAIN, J. E. & BLASIE, J. K. (1972). *Proc. Natl. Acad. Sci. U.S.A.* **69**, 1499–1503.
- LEVINE, Y. K. & WILKINS, M. H. F. (1971). *Nature New Biol.* **230**, 69–72.
- SCHMITT, F. O., BEAR, R. S. & CLARK, G. L. (1935). *Radiology*, **25**, 131–151.
- WEICK, D. (1974). *Biophys. J.* **14**, 233–235.
- WILKINS, M. H. F., BLAUROCK, A. E. & ENGELMAN, D. M. (1971). *Nature New Biol.* **230**, 72–76.
- WORTHINGTON, C. R. & LIU, S. C. (1973). *Arch. Biochem. Biophys.* **157**, 573–579.

Acta Cryst. (1975). **A31**, 15

The Relation between Reduced and Conventional Unit Cells for Centred Monoclinic Lattices

BY HANS GRIMMER*

Battelle, Advanced Studies Center, CH-1227 Carouge-Geneva, Switzerland

(Received 10 April 1974; accepted 25 July 1974)

It is known that 13 among the 44 types of (Niggli) reduced cells correspond to centred monoclinic lattices. For these 13 types, the connexion is given between the reduced cell and a conventional cell. For centred lattices of monoclinic and orthorhombic symmetry, we describe the shape of the conventional cell for the different types of reduced cell. Errors are corrected in the section on *Reduced Cells* of the *International Tables for X-ray Crystallography* [Vol. I (1969), Birmingham: Kynoch Press].

Introduction

In 1928, Niggli described a unique choice of 'reduced' cell among the infinitely many different primitive cells

by which a given lattice can be described. Such a unique choice makes it possible to list the lattice parameters in a standard way also in the case of monoclinic and triclinic crystals. Niggli showed how the Bravais class can be read off the reduced cell, and described the connexion between the reduced cell and a (generally not primitive) conventional cell that respects the lattice symme-

* Present address: Gabelrütteweg 71, CH-3323 Bärswil, Switzerland.